CrystEngComm

PAPER

View Article Online
View Journal | View Issue

Cite this: *CrystEngComm*, 2019, **21**, 6552

The Co^{2+}/Ni^{2+} ion-mediated formation of a topochemically converted copper coordination polymer: structure-dependent electrocatalytic activity†

Pandi Muthukumar, [a] Dohyun Moon *[b] and Savarimuthu Philip Anthony *[a]

Surfactants or templating agents are known to influence the solid-state structural organization of metal–organic coordination polymers. Herein, we report the unusual influence of Co^{2+}/Ni^{2+} ions on the formation of a copper coordination polymeric structure with the *N*-(-2-hydroxybenzyl)-alanine (HBA) ligand. The presence of Ni^{2+} ions in the growth solution led to two different structures: water-coordinated (**1**) and topochemically converted non-water coordinated (**2**) copper coordination polymer structures. On the contrary, the Co^{2+} ions led to only a non-water coordinated topochemically converted structure. X-ray absorption near-edge structure (XANES) and PXRD studies confirmed the absence of Co^{2+}/Ni^{2+} ions in the network and the phase purity of the sample, respectively. The electrocatalytic hydrogen evolution reaction (HER) activity of copper coordination polymers in a basic medium (1.0 M KOH) revealed a relatively enhanced activity for the water-coordinated copper coordination polymer (j_{max} = 220 mA cm^{-2}, η (10 mA cm^{-2}) = 417 mV) as compared to that for the non-water coordinated structure (j_{max} = 84 mA cm^{-2}, η (10 mA cm^{-2}) = 535 mV). However, the mixed catalyst of **1** and **2** exhibited a relatively higher current density (j_{max} = 275 mA cm^{-2}) as compared to the pure water-coordinated polymer (j_{max} = 220 mA cm^{-2}). Importantly, the copper coordination polymer electrocatalyst did not require complementary conducting materials.

Received 29th July 2019,
Accepted 18th September 2019

DOI: 10.1039/c9ce01178a

rsc.li/crystengcomm

Introduction

The crystallization of metal–organic molecules is strongly dependent on various internal and/or external factors including the type of solvent, pH value, metal ions, counter anions, the ligand structure and templating agents.[1–4] For example, self-assembled monolayer (SAM) templates promote the growth of crystals with specific structures, morphologies and orientations.[5–12] SAMs with surface functional groups, such as carboxylic acids, amines and thiols, have been used for the rapid crystallization of amino acids and molecular crystals with polymorphic structures.[13–16] The metal-coordinating surface functionalities of SAMs have also been utilized for fabricating porous metal–organic thin films.[17–19] Plastic, carbon and Langmuir films at the air–water interface have also been explored as templates for the growth of molecular crystals.[20,21] Noncentrosymmetric inorganic crystal templates, such as $KBrO_3$ and $NaBrO_3$, have been shown to promote the growth of noncentrosymmetric polymorphs as compared to that of centrosymmetric polymorphs.[22] Surfactants play an important role in controlling the size, shape and properties of nanocrystals.[23–25] Surfactants serve as a powerful platform in the preparation of new crystalline MOFs with diverse structures as well as in the separation of MOFs with a pure phase *via* competing metal-interacting functionalities.[26–31] Moreover, complete and reversible exchange of metal ions has been demonstrated.[32] Organic ligands can preferably coordinate with a particular metal ion when several metal ions are present in the solution. However, the promotion of metal ion coordination that originates from a metal sheet source by competing metal ions has never been reported. We have been interested in preparing transition metal ion-based coordination polymers *via* water coordination for use as electrocatalysts in the hydrogen evolution reaction (HER). Water-coordinated coordination polymers exhibit enhanced HER activity over non-water coordinated polymers.[33] Since cobalt (Co) and nickel (Ni) ions are cheap earth-abundant metal ions with multiple oxidation states, cobalt (Co) and nickel (Ni)-

[a] *Department of Chemistry, School of Chemical & Biotechnology, SASTRA Deemed University, Thanjavur-613401, Tamil Nadu, India.*
E-mail: philip@biotech.sastra.edu
[b] *Beamline Department, Pohang Accelerator Laboratory, 80 Jigokro-127beongil, Nam-gu, Pohang, Gyeongbuk, Korea. E-mail: dmoon@postech.ac.kr*

† Electronic supplementary information (ESI) available: Electrochemical studies, thermogravimetric data, PXRD, single crystal data and molecular packing. See DOI: 10.1039/c9ce01178a

based materials have drawn significant attention for HER activities.[34–39] Particularly, the direct fabrication of an electrocatalyst on the electrode surface can avoid the use of a binding agent that usually reduces the catalytic activity. We have attempted to grow *N*-(-2-hydroxybenzyl)-alanine (HBA)-based Co and Ni coordination polymers on a copper foil that can be directly used for electrocatalytic studies. HBA, a reduced Schiff base ligand, produced a water-coordinated 1D helical coordination polymer with copper metal ions.[40] The structural arrangement of ligands around the copper metal centre in the coordination polymer has been exploited to demonstrate the topochemical conversion, in which the coordinated water has been replaced by the carbonyl oxygen of carboxylic acid that results in a 3D chiral framework.[40] Hence, we expected a similar water-coordinated coordination network with the Co and Ni metal ions as well and believed that its direct fabrication on a conducting surface could be useful for achieving enhanced electrocatalytic activity. Interestingly, the crystallization of Co^{2+} and Ni^{2+} coordination polymers with the HBA ligand in the presence of copper foil exhibited unusual phenomena. In the presence of Co^{2+} ions, isolated crystals with a clear morphology were completely grown on the copper foil near and above the solution interface, whereas Ni^{2+} produced aggregated crystals only near the solution interface. Single-crystal structure analysis revealed that both crystals were indeed copper-coordination polymers only, and the Co^{2+}/Ni^{2+} metal ions were not included in the network. Furthermore, the presence of Co^{2+} ions led to only a topochemically converted structure (2), whereas Ni^{2+} ions produced both water-coordinated (1) and topochemically converted (2) structures. Controlled studies indicated that the presence of Co^{2+} and Ni^{2+} ions was important for the formation of copper-coordination polymers, and other ions, including $Fe^{2+/3+}$ and Mn^{2+}, could not produce any crystalline materials. Electrocatalytic HER studies of the copper-coordination polymers in a basic medium (1.0 M KOH) showed enhanced activity for the water-coordinated complex as compared to that for the non-water coordinated structure.

Experimental

Copper acetate ($Cu(CH_3COO)_2{\cdot}2H_2O$), cobalt acetate ($Co(CH_3COO)_2{\cdot}4H_2O$), nickel acetate ($Ni(CH_3COO)_2{\cdot}4H_2O$), alanine, lithium hydroxide (LiOH), salicylaldehyde, and Nafion 117 solution were obtained from Merck, India, and used as received. The *N*-(-2-hydroxybenzyl)-alanine (HBA) ligand was synthesised by following a reported procedure.[40]

Co^{2+}/Ni^{2+} ion-induced formation of copper-coordination polymers

Typically, 0.5 g *N*-(-2-hydroxybenzyl)-alanine was dispersed in 5 ml ethanol, and an equivalent amount of $Co(CH_3COO)_2{\cdot}4H_2O/Ni(CH_3COO)_2{\cdot}4H_2O$ was separately dissolved in 5 ml of water. The cobalt solution was slowly added to the ligand and stirred for 1 h. Then, the Cu foil was dipped into this solution and kept for 20 days to obtain dark-coloured crystals on the copper foil surface. Finally, the copper foil was removed, and the crystals were separated, washed with water and allowed to dry.

Characterization

Absorption spectra were obtained using Perkin Elmer 1050. Powder X-ray diffraction (PXRD) was performed using a Bruker instrument, Cu-Kα: λ = 0.1540598 Å. Single crystals were coated with paratone-N oil, and the diffraction data were obtained at 100 K with synchrotron radiation (λ = 0.62998 Å) using the ADSC Quantum-210 detector at 2D SMC with a silicon (111) double crystal monochromator (DCM) at the Pohang Accelerator Laboratory, Korea. For XANES measurements, the crystal was mounted on a loop and scanned for Cu, Co and Ni.

Electrochemical measurements

Electrochemical measurements were performed using a three-electrode system at an electrochemical workstation (CHI660E, Austin, Texas, USA). The three-electrode configuration included a saturated calomel electrode (SCE) as the reference electrode, a graphite rod as the counter electrode, and a modified glassy carbon electrode as the working electrode (GCE, 3 mm diameter). Before surface coating, the GCE was polished using 1 mm, 0.3 mm and 0.05 mm alumina powder, followed by sonication in ethanol and drying in vacuum. The working electrode was fabricated as follows: 4 mg of the electrocatalyst was dispersed in 400 μl ethanol, 100 μl water and 40 μl of 5 wt% Nafion. The mixture was sonicated for 30 min to form a homogenous ink. Finally, 0.3 mg catalyst mixed ink was loaded onto the GCE. Cyclic voltammetry and linear sweep voltammetry at the scan rate of 50 mV s^{-1} were conducted in 1.0 M KOH. For the Tafel plot, the linear portion was fit to the Tafel equation. All the potentials reported in our manuscript were calibrated to a reversible hydrogen electrode (RHE). Electrochemical impedance spectroscopy data were obtained in 1.0 M KOH with frequencies ranging from 0.1 to 100 000 Hz and the amplitude of 10 mV.

Results and discussion

The HBA ligand was synthesised according to a reported procedure.[37] The aqueous mixture of HBA, LiOH and copper acetate produced dark green crystals of the water-coordinated 1D polymer (Scheme 1).[40] The presence of labile coordinated water and the close proximity of the carbonyl oxygen of carboxylic acid in the solid state were exploited to demonstrate the topochemical conversion by heating at 120 °C. The compound lost its single crystalline nature; however, recrystallization from water produced quality crystals that indicated the removal of coordinated water molecules by carbonyl oxygen (Scheme 1).[40] The replacement of Cu^{2+} with Co^{2+}/Ni^{2+} ions is expected to produce similar water-coordinated cobalt/nickel coordination polymer networks, and the immersion of a copper foil would help to grow them directly on a conducting

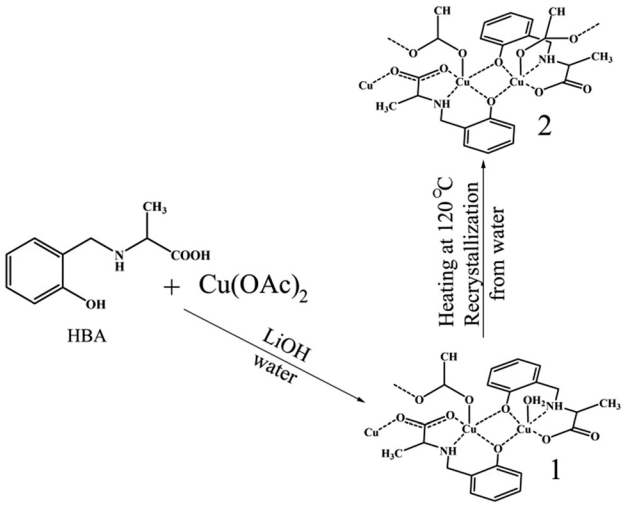

Scheme 1 Synthesis of water-coordinated (**1**) and topochemically converted (**2**) copper-coordination polymers.[40]

surface. However, it did not produce any precipitate or crystals, and the solution remained clear. Hence, under slightly different conditions, the dispersion of the ligand in ethanol and mixing with an aqueous solution of Co^{2+} and Ni^{2+} ions without LiOH were attempted for crystal growth. Copper foil was immersed in the solution and left undisturbed for few days at room temperature (Scheme 2). It was observed that the addition of copper acetate immediately produced precipitates (Fig. S1†). Although it did not produce uniform thin films, Co^{2+} ion-dissolved solution showed the formation of dark-coloured crystals with clear morphology (Scheme 2). Interestingly, all the crystals were grown on the copper foil either at the solution interface or well above the solution. Crystals were grown along the edges of the foil up to the top. The solution appeared clear with a light green colour. On the contrary, the Ni^{2+} ion-dissolved solution produced an aggregated crystalline product along with a precipitate in the solution. The breaking of aggregation clearly showed the formation of clear tiny crystals with similar morphology

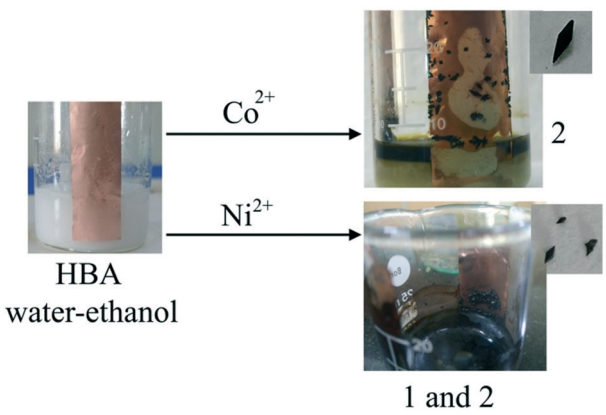

Scheme 2 Images of the growth of **1** and **2** crystals in the presence of Co^{2+}/Ni^{2+} ions.

(Scheme 2). It did not produce any crystals on the top surface of the foil as observed in the case of Co^{2+}. This suggests that Co^{2+} and Ni^{2+} interact differently with the HBA ligand. However, single crystal analysis revealed that only the copper-coordination polymer and no Co^{2+} or Ni^{2+} ions were present in the network (Fig. 1). Furthermore, to confirm the complete absence of Co^{2+} or Ni^{2+} ions in the network solution, X-ray absorption near-edge structure (XANES) analysis was performed for the single crystals, which also clearly showed the presence of only copper (Fig. S2†). The XANES study confirmed the absence of Co^{2+} and Ni^{2+} ions in both crystals.

Surprisingly, the crystals grown from the Co^{2+} ion solution revealed a non-water coordinated copper coordination network structure that perfectly matched the topochemically converted structure (Fig. 1b). Note that the water-coordinated copper coordination polymer has to be heated for 2 h and recrystallized from water to generate topochemically converted non-water coordinated crystals. The perfect match between the PXRD pattern of Co^{2+} ion-grown crystals and the simulated pattern of **2** confirms the phase purity of the sample (Fig. S3†). On the other hand, the crystals grown from the Ni^{2+} ion solution showed both water-coordinated as well as topochemically converted structures (Fig. 1). The PXRD pattern also confirmed the formation of both crystals in the sample (Fig. S3†). Thus, the presence of Co^{2+} ions promoted the formation of the topochemically converted copper-coordination polymer (**2**), whereas the Ni^{2+} ion induced the formation of both water-coordinated (**1**) and topochemically converted (**2**) structures. FTIR analysis also showed a clear difference between **1** and **2**, particularly at the water OH

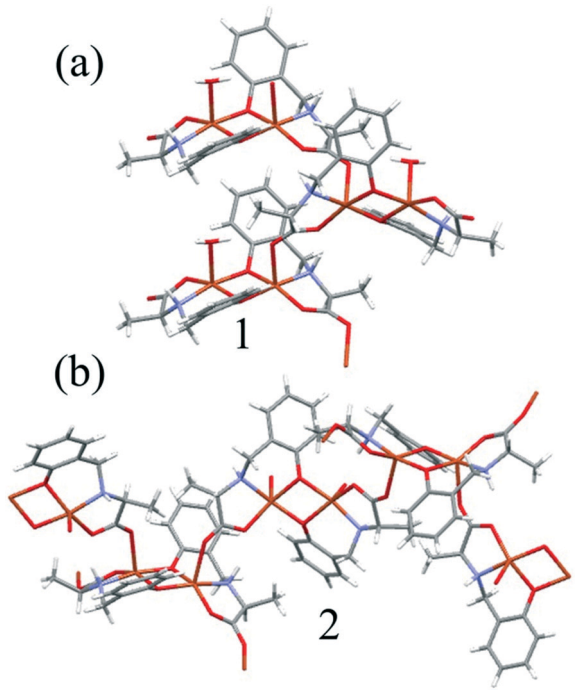

Fig. 1 Different structural motifs of (a) **1** and (b) **2**. C (grey), N (blue), O (red), H (white) and Cu (orange).

stretching position (Fig. S4†). We performed controlled studies to understand the significance of Co^{2+}/Ni^{2+} in the formation of the copper coordination polymer. Compared to the case of copper foil, the addition of the copper acetate salt did not produce any crystalline products in the presence of Co^{2+}/Ni^{2+}. Similarly, there was no crystal formation in the absence of the copper foil. Moreover, the use of other transition metal ions, such as Fe^{2+}, Fe^{3+} and Mn^{2+} ions, instead of Co^{2+}/Ni^{2+} did not produce any crystals or precipitates. The chloride salts of Co^{2+} and Ni^{2+} ions also produced clear crystals on the copper foil (Fig. S5†). Thus, Co^{2+} and Ni^{2+} play a unique role in promoting the formation of the copper-coordination polymer. The mechanism of the Co^{2+}/Ni^{2+} ion-mediated formation of topochemical and water-coordinated polymer is not clear at present. However, the interaction of Co^{2+}/Ni^{2+} ions with the ligand might lead to weak protonation that might oxidise copper in the copper foil and produce crystals. The absorption spectra of HBA with Co^{2+} and Ni^{2+} in an aqueous solution showed a clear absorption change that suggested the interaction of the metal ion with the ligand (Fig. S6†). Thus, to the best of our knowledge, herein, the Co^{2+}/Ni^{2+} ion-mediated formation of an unusual copper coordination polymer was observed for the first time.

Coordination polymer (CP) or metal–organic framework (MOF)-based materials have gained extensive attention for electrocatalytic water splitting.[30,38–40] Particularly, water-coordinated coordination networks exhibit an enhanced hydrogen evolution reaction (HER) when mixed with complimentary conducting materials, such as graphene and acetylene black, at an appropriate ratio.[33,41–47] Recently, we have reported different structural motifs of the copper coordination polymer with the 2,6-pyridinedicarboxylic acid ligand and their structure-dependent HER activity in alkaline and neutral media without the use of complementary conducting materials.[48] Note that the development of an efficient HER electrocatalyst in alkaline or neutral media is highly desired as compared to that of the acidic-medium active catalysts because of the serious environmental problem and corrosive nature of acids. However, water dissociation, an additional step involved in the HER mechanism in alkaline or neutral media, requires higher overpotential as compared to that in an acidic medium.[49] The electrocatalytic HER activities of the water-coordinated copper coordination polymer and topochemically converted non-water coordinated structure-modified glassy carbon electrode were evaluated using electrochemical experiments in an alkaline (pH = 14.0, 1.0 M KOH) medium at the scan rate of 50 mV s^{-1}. The electrode with glassy carbon showed poor HER activity. The water-coordinated coordination polymer (**1**) showed enhanced HER activity as compared to the topochemically converted non-water coordinated coordination polymer. Under the alkaline condition, **1** showed the current density of 220 mA cm^{-2} at the applied potential of 800 mV (Fig. 2a). On the contrary, the non-water coordinated coordination polymer **2** exhibited the current density of 84 mA cm^{-2}. The copper-coordination polymer obtained from the Co^{2+} ion solution also showed a

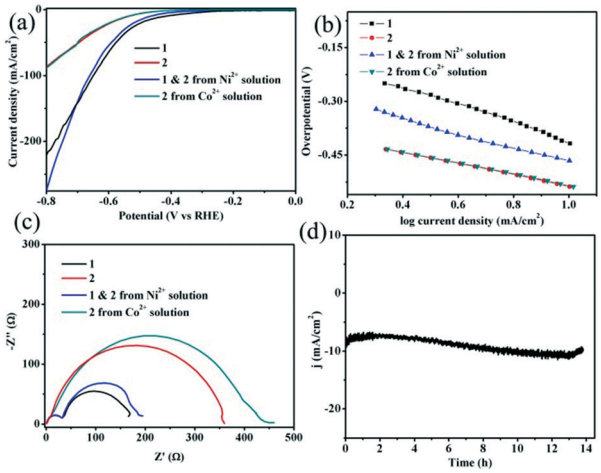

Fig. 2 (a) HER polarization curves, (b) Tafel plots, (c) electrochemical impedance spectroscopy data and (d) current–time chronoamperometric responses of **1** and **2** in 1.0 M KOH.

nearly similar activity and further confirmed the formation of the non-water coordinated structure. Interestingly, the Ni^{2+} ion-mediated crystals that contained both water-coordinated (**1**) and non-water coordinated (**2**) copper polymers exhibited the higher current density of 275 mA cm^{-2} at the applied potential as compared to the case of the pure water-coordinated copper coordination polymer. To achieve the geometric current density of 10 mA cm^{-2}, the water-coordinated copper coordination polymer (**1**) required the lowest overpotential of 417 mV and the mixed catalyst required 465 mV. The coordination polymer **2** needed the highest overpotential of 535 mV to produce the current density of 10 mA cm^{-2}. The Tafel slope is an important property of electrocatalytic materials and used for evaluating the rate-determining step of the HER. Herein, **1** showed the lowest Tafel slope of 98 mV dec^{-1}, and the mixed copper coordination polymer catalysts showed a slightly higher Tafel slope of 121 mV dec^{-1} (Fig. 2b). The topochemically converted structure revealed the highest Tafel slope of 145 mC dec^{-1}. The increased HER electrocatalytic activity of **1** as compared to that of the topochemically converted polymer could be attributed to the presence of a H-bonding functionality such as a water molecule. Note that **1** exhibited strong intermolecular H-bonding in the crystal lattice (Fig. S7†). Hence, the coordinated water molecule in the network structure might form H-bonding with the water solvent that could favour the water dissociation process.[33] The reaction kinetics of the HER electrocatalyst in the acidic medium follows the Volmer pathway by combining the protons from the electrolyte and the electrons from the electrode.[50] However, the reaction starts from water dissociation in basic and neutral media due to the absence of free protons that contribute to low catalytic activity.[51] The Tafel slope of **1** (98 mV dec^{-1}) did not match the Tafel slope of the rate-determining step of Tafel (30 mV dec^{-1}), Heyrovsky (40 mV dec^{-1}) and Volmer (120 mV dec^{-1}) reaction mechanisms in the alkaline medium. This indicates the involvement of

multiple chemical reactions, and the Volmer–Heyrovsky reaction mechanism may be involved at the electrode-catalyst interface during the HER activity;[52] however, the mixed crystals showed a Tafel slope of 121 mV dec^{-1} that perfectly matched with that of the Volmer reaction mechanism; this suggested that water dissociation was the rate-determining step. The comparison of activity indicated that the pure water-coordinated coordination polymer (**1**) required lower overpotential for producing a geometric current density but the mixed form showed higher current density at the applied potential. Furthermore, the electrochemical impedance spectra have been obtained to understand the electrode kinetics of the **1** and **2**-b catalysts (Fig. 2c). The impedance plots of all three polymers are composed of a semicircle in high-frequency regions and a vertical line in low-frequency regions. Charge-transfer resistances clearly differed for water-coordinated and non-water coordinated coordination polymers. Moreover, **1** and **2**-b revealed much lower charge-transfer resistances as compared to the topochemically converted coordination polymer. The relatively low charge-transfer resistance of **1** indicates an efficient electron transfer and favorable HER kinetics at the catalyst/electrolyte interface. The stability study of **1** suggested that the catalyst was stable without a significant loss of activity for over 12 h (Fig. 2d). Thus, **1** was chosen to evaluate its stability due to its relatively higher electrocatalytic activity as compared to that of other polymers. Thus, the present study further substantiates the positive role of water coordination in the electrocatalytic activity of coordination polymers.

Conclusion

In conclusion, the Co^{2+}/Ni^{2+} ions played an unusual role in the formation of a copper coordination polymer, water-coordinated structure and topochemically converted non-water coordinated structure. The Ni^{2+} ions induced the formation of the copper coordination polymeric crystals of **1** and **2**, whereas the Co^{2+} ions mediated the formation of the copper coordination polymeric crystals of only **2**. In the presence of Co^{2+} ions, the crystals were completely formed on the copper foil either at the water–foil interface or above the solution, whereas in the presence of Ni^{2+} ions, the crystals were mostly grown at the interface. Solid-state structural and XANES studies confirmed the absence of both Co^{2+}/Ni^{2+} ions in the coordination network. Thus, the present study indicates that coordinative metal ions can also be used as surfactants or templating agents to control the solid-state structural organization of metal–organic coordination polymers. The electrocatalytic HER studies revealed enhanced activity for the water-coordinated coordination polymer as compared to that for the non-water coordinated structure in the basic medium (1.0 M KOH) without the use of complimentary conducting materials. Moreover, **1** produced the current density of 220 mA cm^{-2} at the applied potential of 800 mV and required an overpotential of 417 mV to produce a geometric current density (10 mA cm^{-2}), whereas **2** showed the current density of 84 mA cm^{-2} and required a higher overpotential (535 mV) to achieve the geometric current density. These results further substantiate the importance of water coordination in coordination polymers for deriving an enhanced electrocatalytic activity in an alkaline medium.

Conflicts of interest

There is no conflicts to declare.

Acknowledgements

Financial support received from the Nanomission, Department of Science and Technology, New Delhi, India (DST-Nanomission scheme no. SR/NM/NS-1053/2015) is acknowledged with gratitude. We thank Dr. P. Suresh kumar for letting us use the electrochemical facility of his lab.

Notes and references

1 C. Janiak, *Dalton Trans.*, 2003, 2781–2804.
2 S. Qiu and G. Zhu, *Coord. Chem. Rev.*, 2009, **253**, 2891–2911.
3 C.-P. Li and M. Du, *Chem. Commun.*, 2011, **47**, 5958.
4 I. Hisaki, N. Ikenaka, N. Tohnai and M. Miyata, *Chem. Commun.*, 2016, **52**, 300–303.
5 R. Hiremath, S. W. Varney and J. A. Swift, *Chem. Mater.*, 2004, **16**, 4948–4954.
6 J. Aizenberg, A. J. Black and G. M. Whitesides, *J. Am. Chem. Soc.*, 1999, **121**, 4500–4509.
7 K. Bandyopadhyay and K. Vijayamohanan, *Langmuir*, 1998, **14**, 6924–6929.
8 J. Küther, R. Seshadri, W. Knoll and W. Tremel, *J. Mater. Chem.*, 1998, **8**, 641–650.
9 K. Naka and Y. Chujo, *Chem. Mater.*, 2001, **13**, 3245–3259.
10 Y. Han, L. M. Wysocki, M. S. Thanawala, T. Siegrist and J. Aizenberg, *Angew. Chem., Int. Ed.*, 2005, **44**, 2386.
11 A. M. Travaille, J. J. J. M. Donners, J. W. Gerritsen, N. A. J. M. Sommerdijk, R. J. M. Nolte and H. van Kempen, *Adv. Mat.*, 2002, **14**, 492–495.
12 Y.-J. Han and J. Aizenberg, *J. Am. Chem. Soc.*, 2003, **125**, 4032–4033.
13 R. Hiremath, J. A. Basile, S. W. Varney and J. A. Swift, *J. Am. Chem. Soc.*, 2005, **127**, 18321–18327.
14 A. Y. Lee, A. Ulman and A. S. Myerson, *Langmuir*, 2002, **18**, 5886–5898.
15 A. L. Briseno, J. Aizenberg, Y.-J. Han, R. A. Penkala, H. Moon, A. J. Lovinger, C. Kloc and Z. Bao, *J. Am. Chem. Soc.*, 2005, **127**, 12164–12165.
16 M. A. Pinard, T. A. J. Grell, D. Pettis, M. Mohammed and K. Aslan, *CrystEngComm*, 2012, **14**, 4557.
17 S. Hermes, F. Schröder, R. Chelmowski, C. Wöll and R. A. Fischer, *J. Am. Chem. Soc.*, 2005, **127**, 13744–13745.
18 F. C. Meldrum, J. Flath and W. Knoll, *Langmuir*, 1997, **13**, 2033–2049.
19 D. Braga, *Angew. Chem., Int. Ed.*, 2003, **42**, 5544–5546.
20 K. Yase, M. Yamanaka, K. Mimura, K. Inaoka and K. Sato, *Appl. Surf. Sci.*, 1994, **75**, 228–232.

21 E. M. Landau, S. G. Wolf, M. Levanon, L. Leiserowitz, M. Lahav and J. Sagiv, *J. Am. Chem. Soc.*, 1989, **111**, 1436–1445.
22 M. J. Prakash, P. Raghavaiah, Y. S. R. Krishna and T. P. Radhakrishnan, *Angew. Chem., Int. Ed.*, 2008, **47**, 3969–3972.
23 W.-W. Xiong, J. Miao, K. Ye, Y. Wang, B. Liu and Q. Zhang, *Angew. Chem., Int. Ed.*, 2014, **53**, 1–6.
24 W.-W. Xiong and Q. Zhang, *Angew. Chem., Int. Ed.*, 2015, **54**, 11616–11623.
25 G. Liu, J. Liu, L. Nie, R. Ban, G. S. Armatas, X. Tao and Q. Zhang, *Inorg. Chem.*, 2017, **56**, 5498–5501.
26 J. Gao, K. Ye, L. Yang, W.-W. Xiong, L. Ye, Y. Wang and Q. Zhang, *Inorg. Chem.*, 2014, **53**, 691–693.
27 J. Gao, K. Ye, M. He, W.-W. Xiong, W. Cao, Z. Y. Lee, Y. Wang, T. Wu, F. Huo, X. Liu and Q. Zhang, *J. Solid State Chem.*, 2013, **206**, 27–31.
28 J. Zhao, Y. Wang, W. Dong, Y. Wu, D. Li, B. Liu and Q. Zhang, *Chem. Commun.*, 2015, **51**, 9479–9482.
29 J. Gao, M. He, Z. Y. Lee, W. Cao, W.- W. Xiong, Y. Li, R. Ganguly, T. Wu and Q. Zhang, *Dalton Trans.*, 2013, **42**, 11367–11370.
30 P. Li, F.- F. Cheng, W.- W. Xiong and Q. Zhang, *Inorg. Chem. Front.*, 2018, **5**, 2693–2708.
31 J. Zhao, X. Liu, Y. Wu, D. S. Li and Q. Zhang, *Coord. Chem. Rev.*, 2019, **391**, 30–43.
32 S. Das, H. Kim and K. Kim, *J. Am. Chem. Soc.*, 2009, **131**, 3814–3815.
33 Y.-P. Wu, W. Zhou, J. Zhao, W.-W. Dong, Y.-Q. Lan, D.-S. Li, C. Sun and X. Bu, *Angew. Chem., Int. Ed.*, 2017, **56**, 13001–13005.
34 M. Chen, J. Qi, W. Zhang and R. Cao, *Chem. Commun.*, 2017, **53**, 5507–5510.
35 J. Wang, S. Mao, Z. Liu, Z. Wei, H. Wang, Y. Chen and Y. Wang, *ACS Appl. Mater. Interfaces*, 2017, **9**, 7139–7147.
36 J. Wang, Z. Wei, H. Wang, Y. Chen and Y. Wang, *J. Mater. Chem. A*, 2017, **5**, 10510–10516.
37 J.-X. Feng, S.-Y. Tong, Y.-X. Tong and G.-R. Li, *J. Am. Chem. Soc.*, 2018, **140**, 5118–5126.
38 W. Zhou, X.-F. Lu, J.-J. Chen, T. Zhou, P.-Q. Liao, M. Wu and G.-R. Li, *ACS Appl. Mater. Interfaces*, 2018, **10**, 38906–38914.
39 D. Yan, R. Chen, Z. Xiao and S. Wang, *Electrochim. Acta*, 2019, **303**, 316–322.
40 J. D. Ranford, J. J. Vittal, D. Wu and X. Yang, *Angew. Chem., Int. Ed.*, 1999, **38**, 3498–3501.
41 M. Jahan, Z. Liu and K. P. Loh, *Adv. Funct. Mater.*, 2013, **23**, 5363–5372.
42 X. Wang, W. Zhou, Y.-P. Wu, J.-W. Tian, X.-K. Wang, D.-D. Huang, J. Zhao and D.-S. Li, *J. Alloys Compd.*, 2018, **753**, 228–233.
43 J.-W. Tian, M.-X. Fu, D.-D. Huang, X.-K. Wang, Y.-P. Wu, J. Y. Lu and D.-S. Li, *Inorg. Chem. Commun.*, 2018, **95**, 73–77.
44 X. Li, H. Lei, X. Guo, X. Zhao, S. Ding, X. Gao, W. Zhang and R. Cao, *ChemSusChem*, 2017, **10**, 4632–4641.
45 W. Zhou, Y.-P. Wu, X. Wang, J.-W. Tian, D.-D. Huang, J. Zhao, Y.-Q. Lan and D.-S. Li, *CrystEngComm*, 2018, **20**, 4804–4809.
46 X. Li, H. Lei, J. Liu, X. Zhao, S. Ding, Z. Zhang, X. Tao, W. Zhang, W. Wang, X. Zheng and R. Cao, *Angew. Chem., Int. Ed.*, 2018, **57**, 15070–15075.
47 H. Li, X. Li, H. Lei, G. Zhou, W. Zhang and R. Cao, *ChemSusChem*, 2019, **12**, 801–806.
48 P. Muthukumar, D. Moon and S. P. Anthony, *Catal. Sci. Technol.*, 2019, **9**, 4347–4354.
49 N. Mahmood, Y. Yao, J.-W. Zhang, L. Pan, X. Zhang and J.-J. Zou, *Adv. Sci.*, 2018, **5**, 1700464.
50 B. E. Conway and B. V. Tilak, *Electrochim. Acta*, 2002, **47**, 3571–3594.
51 Y. Jiao, Y. Zheng, M. Jaroniec and S. Z. Qiao, *Chem. Soc. Rev.*, 2015, **44**, 2060–2086.
52 W. F. Chen, S. Iyer, S. S. Iyer, K. Sasaki, C. H. Wang, Y. Zhu, J. T. Muckerman and E. Fujita, *Energy Environ. Sci.*, 2013, **6**, 1818–1826.